RAPID COMMUNICATIONS

PHYSICAL REVIEW B VOLUME 49, NUMBER 2 1 JANUARY 1994-II

Direct evidence of phase separation in as-deposited Fe(Co)-Ag films with giant magnetoresistance

H. Wan, A. Tsoukatos, and G. C. Hadjipanayis
Department of Physics and Astronomy, University of Delaware, Newark, Delaware 19716

Z. G. Li
DuPont Company, P. O. Box 80356, Wilmington, Delaware 19880-0356

J. Liu
CSSS, Center for Solid State Electronics, Arizona State University, Tempe, Arizona 85287
(Received 27 September 1993)

High-resolution analytical electron microscopy (EM) on as-deposited dilute Fe(Co)-Ag films showed Fe(Co) clusters embedded in a Ag matrix suggesting that these materials are not uniform substitutional alloys as it was previously believed. The cluster sizes observed from the EM images are slightly larger than those calculated from magnetization curves, and this has been attributed to the interface roughness existing between the magnetic clusters and the nonmagnetic matrix. The magnetic properties and magnetoresistance values in these films are also discussed relative to the high-resolution electron-microscopy results.

The solubility of Fe and Co in Ag is rather negligible, and no equilibrium alloys or compounds exist in the Fe-Ag and Co-Ag binary phase diagrams. However, the high quenching rate during the vapor-deposition process may result in metastable alloys at room temperature or cryogenic temperatures.[1] In the past several studies including ours[2–4,7] in Fe(Co)-Ag granular films claimed a uniform substitutional alloy with a fcc structure and magnetic properties similar to those of a spin glass. Recently, Fe(Co)-Ag as well as Co-Cu single-layer composite films were found to have giant magnetoresistance (GMR), in both the as-made and annealed states,[5–7] which is not consistent with the spin glass picture and raised again the question about the phase constitution and structure of these alloys.

GMR was first discovered in Fe/Cr multilayer systems[8] and later in other systems including Co/Cu, Co/Ag, and Co/Ru multilayers.[9,10] The resistance of multilayers is high when the adjacent magnetic layers are coupled antiferromagnetically, and it is decreased substantially when the magnetic moments are aligned parallel by an applied magnetic field. Theoretical models attribute GMR to spin-dependent interfacial and bulk scattering,[11–14] where the effect of roughness at the interfaces of the layered structures has also been examined.[13] The GMR studies on single-layer films strongly suggest that the GMR is related to the heterogeneous magnetic structure consisting of small magnetic entities embedded in a nonmagnetic matrix. The homogeneous substitutional alloy picture in Fe(Co)-Ag single-layer films is not consistent with the GMR behavior of these films

In the work presented here, we have used scanning transmission and conventional transmission electron microscopy to study the microstructure of as-deposited (Fe,Co)-Ag granular films and correlate it with their magnetotransport properties. We have found that the as-made Fe(Co)-Ag films are not homogeneous but phase separated materials, even though conventional x-ray and electron diffraction show only a single fcc structure. The average size of magnetic particles as well as the distance between the particles have been determined from analytical electron-microscopy (EM) studies and were found to be comparable to those estimated from the magnetization and susceptibility data.

$(Fe,Co)_xAg_{1-x}$ ($x=0.1-0.6$) films were fabricated via dc magnetron sputtering using the tandem deposition method. The water cooled substrate platform was rotated between the two guns through a computer controlled stepper motor. The base pressure was approximately 5×10^{-8} Torr, and the Ar gas pressure during deposition was 5–10 mTorr. Each sample was about 200 nm thick.

The composition and thickness of the films were determined by Rutherford backscattering spectroscopy (RBS). A superconducting quantum interference device magnetometer was used for the magnetic measurements, and the magnetoresistance was measured using the four-probe technique, with the applied field current parallel to the longitudinal axis of the rectangular shaped specimens. A Phillips 3100 x-ray-diffraction unit was used to study the crystal structure. A VG HB 501 (100 KV) microscope was used for high-angle annular dark-field (HAADF) and energy dispersed spectroscopy (EDS) studies in which chemical analysis can be obtained at a spot size of about 1 nm.

The magnetoresistance behavior in the as-deposited Fe-Ag and Co-Ag films is quite similar, as reported in our previous papers.[7,15] GMR was found to depend strongly on composition; it initially increased with the Fe(Co) content, reaching the peak values of 15% and 30% for 25 at % Fe and 35 at % Co, respectively, and then it disappeared at about 60 at % Fe(Co) (Fig. 1). The GMR also shows a strong dependence on temperature with the highest values obtained at cryogenic temperatures. The deposition conditions such as the deposition rate were found to affect the resulting GMR values substantially.[15]

Figure 2 shows the x-ray diffraction patterns of as-

0163-1829/94/49(2)/1524(4)/$06.00

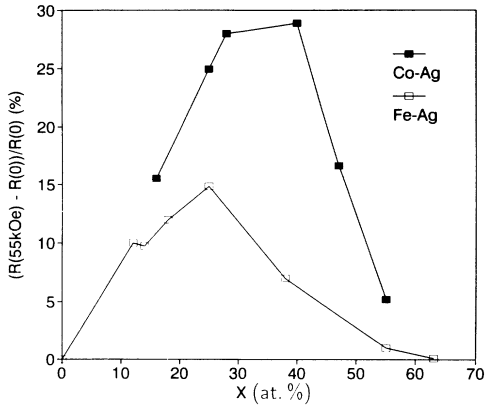

FIG. 1. Longitudinal magnetoresistance as a function of composition in as-made $Fe(Co)_xAg_{1-x}$ films at 30 K.

deposited Co_xAg_{1-x} samples with different compositions. The samples with x up to 40 at % show only one set of fcc structure peaks with a lattice constant close to pure Ag. The (111) Ag peak is found to be slightly shifted to higher angles (1.4%) with increasing Co, indicating a decrease in d spacing. The shift in (111) is so small that it cannot directly be related to a Co-Ag alloy with similar composition; it is probably due to mismatch and boundary effects in the Co and Ag cluster interfaces. The width of the (111) peak is increased with the Co content, indicating that the Ag grain size becomes smaller, and that the distance between the Co clusters is changed in the same way, since the Co cluster density is expected to increase with higher Co contents. Similar results have been observed in Fe-Ag films. The shift in the (111) Ag peak is about 0.7% for the Fe_xAg_{1-x} samples with x up to 36%, and the existence of a uniform Fe-Ag alloy can be similarly excluded. In addition, the (200) line for fcc Ag (2.044 Å) overlaps with both the fcc Co(111) line (2.0467 Å) and the bcc Fe (110) line (2.0268 Å), and this poses a difficulty in making a definite conclusion about phase separation from x-ray-diffraction (XRD) data.

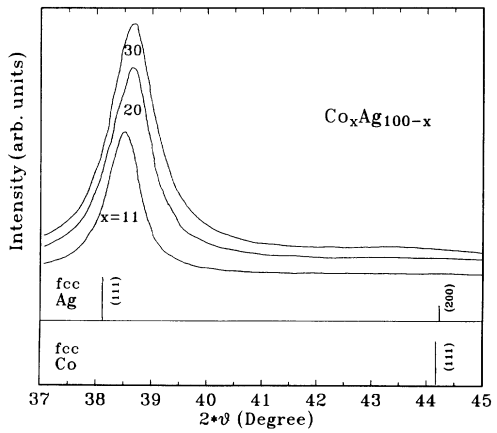

FIG. 2. X-ray-diffraction spectra of Co_xAg_{100-x} films. The XRD curves have been shifted to allow observation of the individual spectra.

Electron microscopy investigations were performed on thick and thin, as well as on Si_3N_4-coated Fe(Co)-Ag films. The best images were achieved in very thin, just-continuous Fe(Co)-Ag films; in thicker films, many different particles were superimposed in the two-dimensional image of the electron microscope, thus making impossible their individual chemical composition identification using the EDS technique. Ion thinning was not used in order to avoid post deposition induced artifacts in the samples. The main structural characteristics of these films were very similar, showing a fine grain fcc structure with sizes in the range of 1–5 nm. The high-angle annular dark-field scanning transmission electron-microscopy (STEM) image of as-deposited Fe-Ag films clearly showed phase separated Fe and Ag particles with different contrast (Fig. 3). The gray and white areas shown in Fig. 3 were examined with EDS using a 1 nm electron beam and were identified as Fe and Ag, respectively. The Fe particles are not uniformly distributed, having an ellipsoidal shape, and a Gaussian size distribution with an average size about 1.5 nm. The Ag particles have distinct large and small sizes with the large size about 15 nm and the small size about 2 nm. Nanodoffraction on the large and small Ag particles shows that they are fcc Ag crystals. The Fe particles did not show any crystal diffraction spots, probably because of a lower crystalline order of the nanosized clusters. This may be the main reason why x-ray and electron diffraction patterns show only one set of fcc peaks. Details of the microstructure and atomic resolution TEM results will be published separately.[16]

Direct current susceptibility measurements show that the Fe(Co) diluted Fe(Co)-Ag samples with a large GMR value have a peak in zero-field-cooled (ZFC) curves (Fig. 4). This behavior is characteristic of both spin glasses and superparamagnetic particles. To distinguish between these two cases, magnetization curves at different temperatures have been examined. Above the peak temperature, a nonlinear universal M-vs-H/T curve is observed (Fig. 5), typical of superparamagnetic particles; below the peak temperature, a sharp rise in the magnetization at low fields indicates ferromagnetism. The slope at high magnetic fields could be the result of the paramagnetic behavior of the surface spins in Fe(Co) clusters, due to the lack of enough Fe(Co) neighbors at surfaces or to the pinning of the surface spins in the cluster. The peak temperature is identified as the blocking temperature T_B, and as expected it depends strongly on the cluster size. The higher blocking temperature of the $Fe_{25}Ag_{75}$ film reveals that the average Fe cluster size is larger than that of the $Fe_{18}Ag_{82}$ sample. The $Fe_{18}Ag_{82}$ sample has a sharp peak, indicating a nearly uniform Fe cluster size. In the $Fe_{25}Ag_{75}$ sample, a broad peak is observed indicating a distribution in Fe cluster size. However, from these curves it is difficult to quantitatively analyze the cluster size, because of the lack of anisotropy data and information about the cluster shape. The cluster size was estimated indirectly from the average effective magnetic moment μ_{eff} of clusters calculated by fitting the $M(H)$ curves above the blocking temperature (T_B) to the Langevin function $L(a)$:

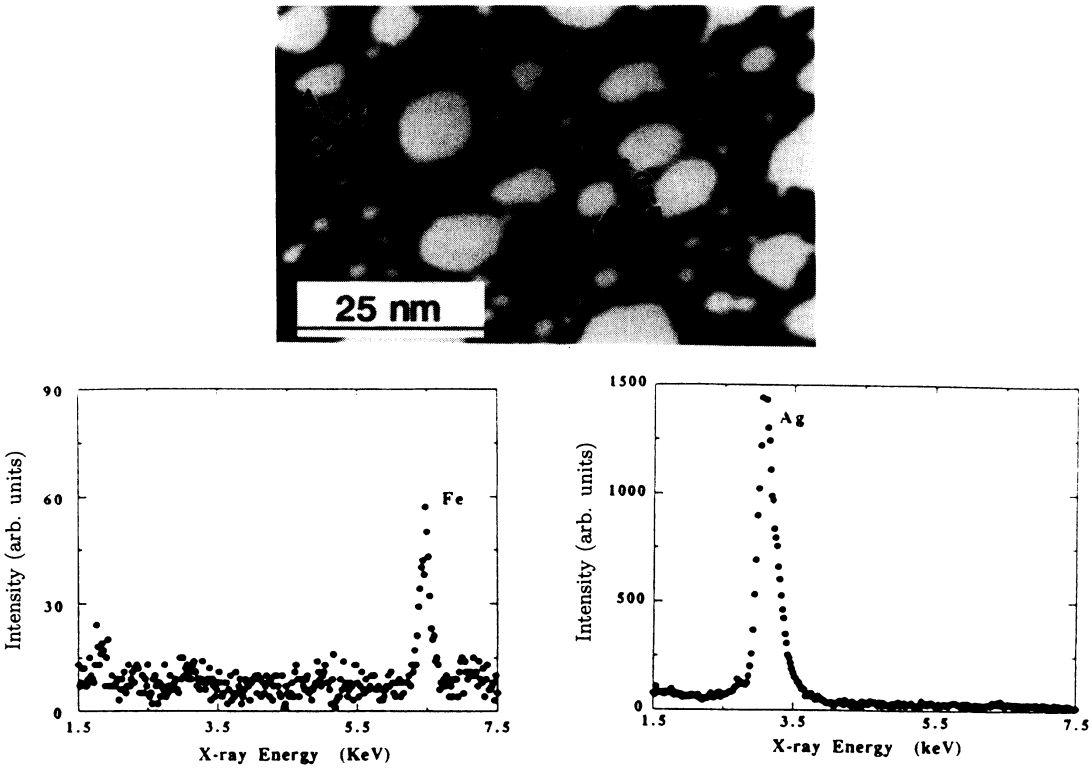

FIG. 3. $Fe_{25}Ag_{75}$ STEM image; the Fe and Ag energy dispersive spectra were obtained from the gray and white spots, respectively.

$$M/M_0 = L(a) = \coth(a) - (1/a) ,$$

where $a = \mu_{\text{eff}} H/kT$. The results show a magnetic moment (μ_{eff}) much larger than the atomic Fe and Co moments, consistent with the cluster picture. For example, $\mu_{\text{eff}} = 197\mu_B$ for $Fe_{18}Ag_{82}$ and $427\mu_B$ for $Fe_{25}Ag_{75}$. If $2.2\mu_B$ is used as the magnetic moment per Fe atom in the cluster, the number of atoms in the cluster is about 94 and 203 for $Fe_{18}Ag_{82}$ and $Fe_{25}Ag_{75}$ samples, respectively. Assuming spherically shaped clusters this would correspond to a size of about 1.3 nm for the $Fe_{18}Ag_{82}$ sample. The clusters are larger in Fe(Co)-rich samples as expected. The size of these clusters is slightly smaller than that from our EM results, and this may be due to the surface atoms not contributing to the magnetic moment of the cluster.

The cluster picture of our films is also consistent with the field dependence of magnetoresistance, which is found to follow a quadratic dependence on the average magnetization of the assembly (Fig. 6), as predicted for single-domain ferromagnetic particles in a nonmagnetic matrix[17]

$$R(H) = \frac{\rho(H) - \rho(H_s)}{\rho(H_s)} = \frac{\rho_2^2}{\rho_1^2 - \rho_2^2}[1 - \alpha^2(H)] = \beta_0[1 - \alpha^2(H)] .$$

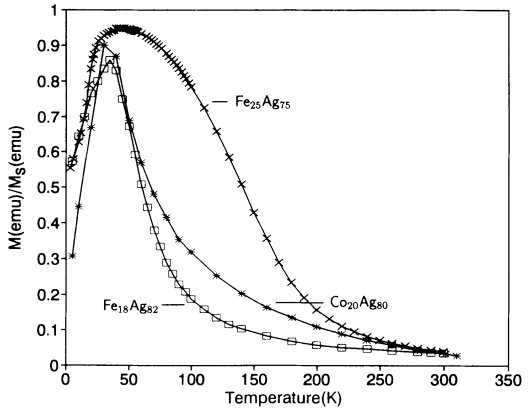

FIG. 4. Zero-field-cooled magnetization as a function of temperature, with external field $H_{\text{ext}} = 50$ and 100 Oe for Co-Ag and Fe-Ag films, respectively.

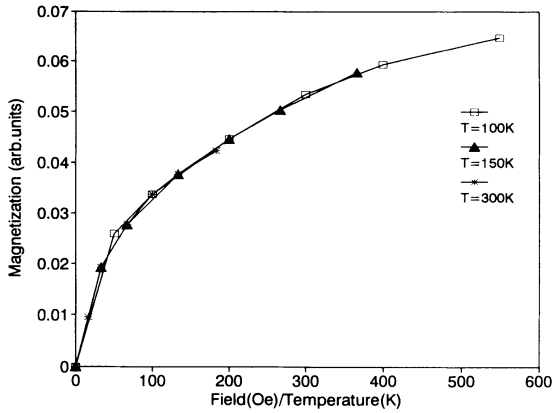

FIG. 5. Magnetization curves of $Fe_{18}Ag_{82}$ film at different temperatures, plotted as a function of H/T above the blocking temperature.

$R(H)=\Delta\rho/\rho$ is maximum for $H=H_c$ and $\alpha=M(H)/M_s=0$.

It is difficult to calculate the GMR of our films quantitatively, because of the particle size distribution. The state of the clusters could vary from superparamagnetic to single domain and may even become multidomain in the high ferromagnetic content range. For very dilute Fe(Co) samples, the cluster sizes are well below the critical size for superparamagnetic behavior and at the measuring temperature of 20 K, the applied magnetic field (55 kOe) is not enough to align the moment of all the clusters. With increasing Fe(Co) content, most of the particles become larger, possibly near the single-domain particle size. Their moments are easier to align and correspondingly the GMR measured are larger. Further increase in the Fe(Co) content may increase the GMR because of easier saturation. However, according to Zhang and Levy's theory,[17] the GMR is expected to decrease with increasing particle size, and this explains the maxima observed in the GMR values at $Co_{35}Ag_{65}$ and $Fe_{25}Ag_{75}$.

The results of these studies have shown clearly that as-deposited Fe(Co)-Ag films are not uniform substitutional alloys, as was believed before but, rather inhomogeneous films consisting of small Co(Fe) entities randomly distributed in the Ag matrix. This picture is consistent with the GMR and its field dependence in these films. It is also in agreement with the thermomagnetic data and the field dependence of magnetization (Langevin function) above the blocking temperature.

Based on these results our future optimization studies will focus on the deposition conditions to obtain better size and cluster uniformity which will hopefully lead to optimized magnetoresistance and to a shift in the GMR maximum to a higher Fe(Co) content that can possibly contribute to a reduction in the saturation field.

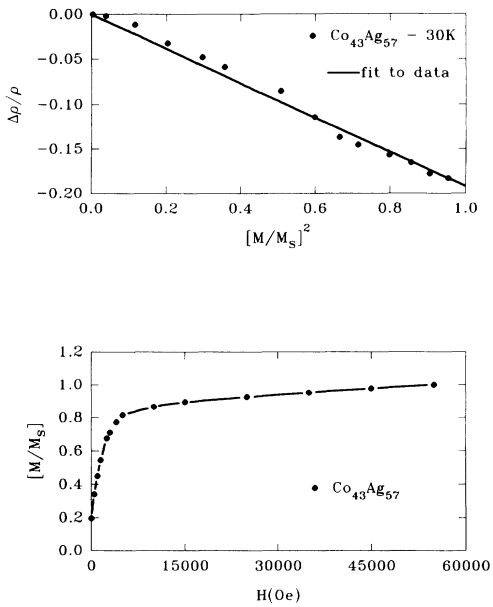

FIG. 6. The quadratic dependence of magnetoresistance on the average magnetization of the assembly. The corresponding normalized magnetization curve is also shown as a function of applied field at 30 K.

This work was supported by NSF Grant No. DMR 8917028.

[1]Y. Nakamura, K. Sumiyama, and N. Kataoka, Hyperfine Interact. **28**, 1029 (1986).

[2]J. R. Childress and C. L. Chien, Phys. Rev. B **43**, 8089 (1991).

[3]J. A. Barnard, A. Waknis, M. Tan, E. Haftek, M. R. Parker, and M. L. Watson, J. Magn. Magn. Mater. **114**, L230 (1992).

[4]J. Q. Xiao, J. S. Jiang, and C. L. Chien, Phys. Rev. B **46**, 9266 (1992).

[5]A. Berkowitz, A. P. Young, J. R. Mitchell, S. Zhang, M. J. Carey, F. E. Spada, F. T. Parker, A. Hutten, and G. Thomas, Phys. Rev. Lett. **68**, 3745 (1992); Appl. Phys. Lett. **61**, 2935 (1992); J. Appl. Phys. **73**, 5320 (1993).

[6]J. Q. Ziao, J. S. Jiang, and C. L. Chien, Phys. Rev. Lett. **68**, 3749 (1992).

[7]A. Tsoukatos, H. Wan, G. C. Hadjipanayis, and Z. G. Li, Appl. Phys. Lett. **61**, 3059 (1992).

[8]M. N. Baibich, J. M. Broto, A. Fert, F. Nguyen Van Dau, F. Petroff, P. Etienne, G. Creuzet, A. Friederich, and J. Chazelas, Phys. Rev. Lett. **61**, 2472 (1988).

[9]J. J. Krebs, P. Lubitz, A. Chaiken, and G. A. Prinz, Phys. Rev. Lett. **63**, 1645 (1989).

[10]S. S. Parkin, R. Bhadra, and K. P. Roche, Phys. Rev. Lett. **66**, 2152 (1991).

[11]P. M. Levy, S. Zhang, and A. Fert, Phys. Rev. Lett. **65**, 1643 (1990).

[12]R. E. Camley and J. Barnes, Phys. Rev. Lett. **63**, 664 (1989).

[13]R. F. Carcia and A. Suna, J. Appl. Phys. **54**, 2000 (1983).

[14]Shufeng Zhang, Appl. Phys. Lett. **61**, 1855 (1992).

[15]A. Tsoukatos, H. Wan, G. C. Hadjipanayis, and K. R. Lawless, IEEE Trans. Magn. (to be published).

[16]Z. G. Li, H. Wan, J. Liu, A. Tsoukatos, G. C. Hadjipanayis, and L. Liang, Appl. Phys. Lett. (to be published).

[17]Shufeng Zhang and P. M. Levy, J. Appl. Phys. **73**, 5315 (1993).

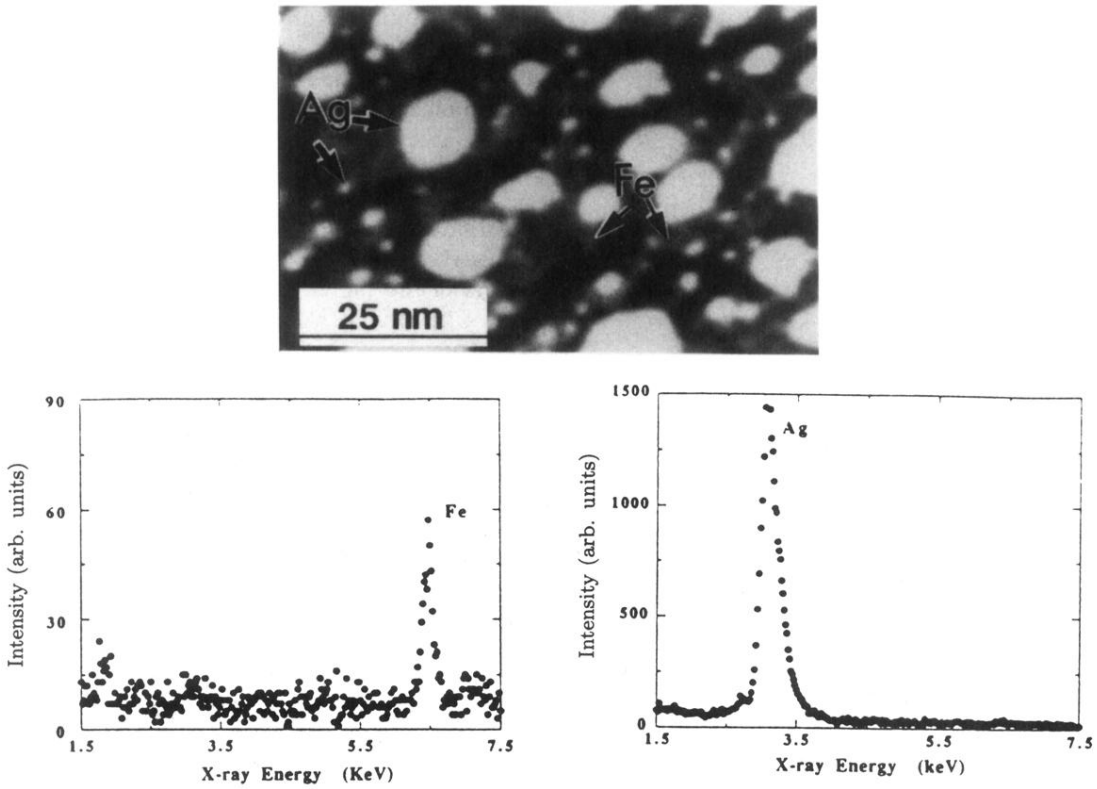

FIG. 3. $Fe_{25}Ag_{75}$ STEM image; the Fe and Ag energy dispersive spectra were obtained from the gray and white spots, respectively.